Shifts in ENSO coupling processes under global warming

Sjoukje Philip[1] and Geert Jan van Oldenborgh[1]

Received 2 March 2006; revised 1 May 2006; accepted 3 May 2006; published 8 June 2006.

[1] Global warming may shift the properties and dynamics of El Niño. We study the shifts in ENSO couplings in IPCC-AR4 coupled general circulation climate models. First, we compare period, pattern, amplitude and mean state of the Pacific Ocean between the current climate and a high CO_2 climate. Next, shifts in ENSO couplings between sea surface temperature (SST), thermocline depth and wind stress are discussed. Although the mean state shifts, the overall ENSO properties do not change much. Changes in the mean state affect the feedback loop. Higher mean SST provides higher damping through cloud feedback. The shallower thermocline and mixed layer depth increase SST sensitivity to thermocline variability and wind stress. Wind response to SST variability increases where the mean SST has increased the most. However, the higher damping and more stable atmosphere compensate the other changes and the residual change in ENSO properties is relatively small. **Citation:** Philip, S. Y., and G. J. van Oldenborgh (2006), Shifts in ENSO coupling processes under global warming, *Geophys. Res. Lett.*, *33*, L11704, doi:10.1029/2006GL026196.

1. Introduction

[2] El Niño — Southern Oscillation (ENSO) is a climate phenomenon that affects large parts of the world. It is therefore important to gain more insight into the behaviour of El Niño in a future, warmer climate. Projections of the properties of ENSO in a future climate are made with general circulation models (GCMs). Most models that describe ENSO reasonably well in the current climate show only small changes in the behavior of ENSO. This can be the result of two very different scenarios: either the strength of the couplings remains similar to the current values in spite of the changing background state, or they change in such a way that the effects cancel in overall ENSO properties.

[3] Recently, mean state, period, pattern and amplitude of ENSO in an enhanced greenhouse gas (GHG) scenario of the IPCC-AR4 GCMs have been analyzed [e.g., *Guilyardi*, 2006; *Merryfield*, 2006; *Van Oldenborgh et al.*, 2005]. *Guilyardi* [2006] analyzed the ENSO amplitude and frequency and found no consistency in changes in a GHG scenario in a range of GCMs, although he did find a trend to a more thermocline-driven mode. Furthermore, he showed that a higher El Niño amplitude is related to a weaker mean zonal wind stress (τ_x). The relationship between ENSO period and the pattern of the anomalous zonal wind stress has been examined by *Kirtman* [1997], *Zelle et al.* [2005], and *Capotondi et al.* [2006]. They have shown that a broader meridional pattern is associated with longer periods. *Capotondi et al.* [2006] have also examined the dependency of the ENSO period upon the longitudinal position of the wind stress, and have shown that models with westward displaced anomalous wind stresses tend to have a shorter period. *Merryfield* [2006] linked changes in sea surface temperature (SST) to changes in SST variability. His results indicate that a higher mean SST or a stronger temperature difference between east and west intensify SST variability. *Van Oldenborgh et al.* [2005] investigated the feedback loop between SST, wind stress and thermocline depth in the current climate, and this allowed them to identify a subset of six most reliable models. In these models they showed that the mean sea level pressure (SLP) state and amplitude of ENSO do not change much in a GHG scenario.

[4] In this study we investigate whether and how the underlying mechanisms of ENSO change. We analyze for GCMs the feedback loop between SST, thermocline depth and wind stress as defined by *Van Oldenborgh et al.* [2005]. We compare a GHG scenario with the 20th century, and investigate the connection with changes in mean states of SST, thermocline and wind stress. Furthermore, we connect changes in the feedback loop and mean states to changes in ENSO pattern, amplitude and period.

2. Models

[5] The set of models we use in this study is a selection of the AR4 climate models that were available via the IPCC data centre. The selection consists of ECHAM5/MPI-OM (ECHAM5), GFDL-CM2.0 (GFDL2.0), GFDL-CM2.1 (GFDL2.1), MIROC3.2(medres) (MIROC) and UKMO-HadCM3 (HadCM3). These models have enough data available for the GHG scenario (sresa1b), with a doubling of CO_2 up to 2100 and stabilisation afterward, and they were shown by *Van Oldenborgh et al.* [2005] to have the most realistic description of the mechanisms of ENSO in both pattern and feedback strength in the current climate. The simulation for the current climate (20c3m) has been used by *Van Oldenborgh et al.* [2005]. The period used for the warmer climate is 2200–2300 except for HadCM3 where we used 2100–2200, since the period 2200–2300 was not available.

3. Overall Properties

[6] First, we analyze the overall properties of ENSO where we compare the differences between the current climate and a climate with doubled CO_2 concentration. Besides period, pattern and amplitude we will also analyze the mean states of SST, zonal wind stress, thermocline depth and mixed layer depth (MLD).

[1]Royal Netherlands Institute of Meteorology, De Bilt, Netherlands.

0094-8276/06/2006GL026196$05.00

Table 1. Amplitude 20th Century and Relative Change in Amplitude Between the 20th and 23rd Centuries of SST in the NINO3, the NINO3.4 and the NINO4 Regions

Model	Scenario	NINO3	NINO3.4	NINO4
ECHAM5	20c3m	1.34 ± 0.04	1.41 ± 0.05	1.23 ± 0.04
	change	+10% ± 8%	+22% ± 8%	+27% ± 8%
GFDL2.0	20c3m	0.97 ± 0.07	1.05 ± 0.08	0.94 ± 0.07
	change	+4% ± 12%	+2% ± 13%	−14% ± 13%
GFDL2.1	20c3m	1.29 ± 0.12	1.33 ± 0.12	1.16 ± 0.09
	change	−14% ± 14%	−17% ± 14%	−28% ± 12%
HadCM3	20c3m	0.94 ± 0.05	0.99 ± 0.06	0.87 ± 0.05
	change	−5% ± 11%	+7% ± 11%	+22% ± 9%
MIROC	20c3m	0.52 ± 0.03	0.54 ± 0.04	0.52 ± 0.03
	change	−23% ± 9%	−17% ± 10%	−15% ± 9%

3.1. Period, Pattern and Amplitude

[7] The pattern and period of ENSO are defined as the first EOF of SST and the full width at half height of the spectrum of the principal component of the leading EOF. The changes in pattern and period between a current and a future climate are very small [e.g., *Van Oldenborgh et al.*, 2005; *Guilyardi*, 2006; *Merryfield*, 2006; *Toniazzo*, 2006].

[8] The amplitude of El Niño is defined as the standard deviation of SST in a 5°S–5°N region in the Pacific Ocean. The amplitudes in the NINO3 (150°W–90°W), NINO3.4 (170°W–120°W) and NINO4 (160°E–150°W) regions show no consistent change (see Table 1). This is consistent with earlier results [*Van Oldenborgh et al.*, 2005; *Guilyardi*, 2006; *Merryfield*, 2006; *Toniazzo*, 2006]. The amplitude in the MIROC model is quite small and the pattern extends too far to the west. The skewness is not considered since this property is not modelled well.

[9] Overall, the changes in these ENSO properties are not large.

3.2. Mean States

[10] Comparing the 20th and the 23rd century, the mean SST rises more at the equator than in the subtropics, see also *Liu et al.* [2005], Figure 1. For GFDL2.0 and GFDL2.1 this rise is about the same in the central Pacific and the coastal zone in the east. ECHAM5 and HadCM3 show a higher increase in temperature in the east than in the west. The warming in MIROC corresponds clearly with the ENSO pattern in SST. However, only ECHAM5 and MIROC show a significant shift in SLP pattern in sresa2 2050–2100, towards a pattern that resembles an El Niño event [*Van Oldenborgh et al.*, 2005].

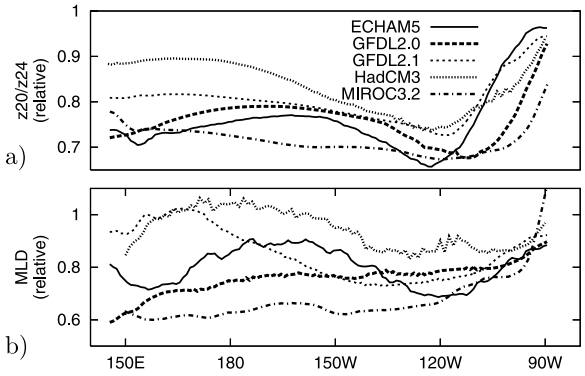

Figure 1. Relative change in (a) thermocline depth approximated by z_{20} (20th century) and z_{24} (23rd century) and (b) mixed layer depth, estimated by the average of the monthly values of z(SST-0.5).

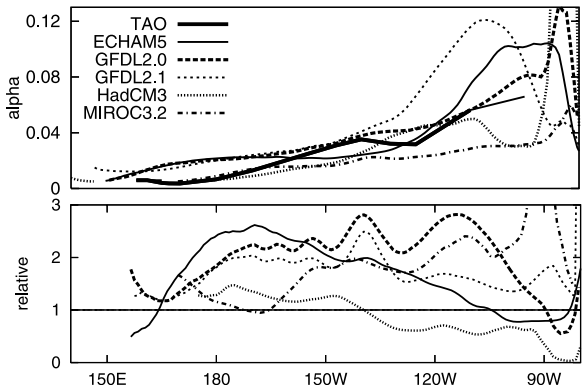

Figure 2. Sensitivity of SST to thermocline variability α [Km^{-1}] for the 20c3m scenario and the relative change in the warmer climate.

[11] In all models the mean zonal wind stress between 10°S–10°N becomes weaker (0–40%) in the 23rd century (not shown). It also becomes more symmetrical around the equator and the area of convection shifts somewhat to the east.

[12] As an approximation for the thermocline, the division between warm and cold water, we use an isotherm. For all five models z_{24} (23rd century) or z_{20} (20th century) is a good approximation for the maximum gradient of the thermocline. The approximation becomes less accurate west of 160°W where the thermocline becomes more diffuse but also less important for the coupling with the atmosphere due to the deeper mean location. We checked for one model (GFDL2.1) that the maximum gradient of the thermocline behaves the same as in the TAO observations [*McPhaden et al.*, 1998], namely a trend to smaller maximum gradients during La Niña. Except for HadCM3, where the thermocline depth remains about the same, the whole thermocline shoals in a warmer climate, and shoals more in the west, see Figure 1a. The reduction of the thermocline slope is directly related to the weaker mean zonal wind stress that is observed in all models.

[13] Another result of the weaker mean zonal wind stress is the reduction in MLD, see Figure 1b. Due to the weakened wind and stronger stratification the depth of the mixed layer decreases.

[14] In general, we see that in a warmer climate the mean state of the Pacific ocean changes considerably.

4. ENSO Mechanisms

[15] So far, we discussed the gross characteristics of ENSO. We find that although mean states do change considerably, changes in ENSO properties are small. In order to understand why these changes are so small we investigate the mechanisms behind them. The most important mechanisms that affect El Niño are the SST response to thermocline and wind variabilities and the wind response to SST perturbations.

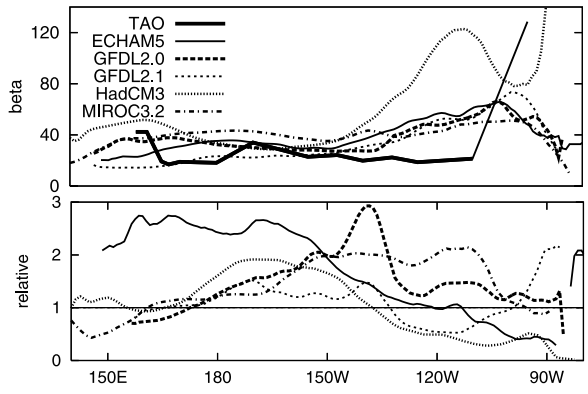

Figure 3. Sensitivity of SST to wind stress variability β [KPa^{-1}] for the 20c3m scenario and the relative change in the warmer climate.

4.1. SST Variability

[16] First we examine SST variability caused by thermocline anomalies, wind stress anomalies and damping. SST anomalies can be fitted with a simple SST equation [*Burgers and van Oldenborgh*, 2002],

$$\frac{dT}{dt}(x,y,t) = \alpha(x,y)\, z_{20/24}(x,y,t-\delta) + \beta(x,y)\, \tau_x(x,y,t) - \gamma(x,y)\, T(x,y,t), \quad (1)$$

that explains about 60–80% of the total variance in the TAO data and all five models. T is the local SST, $z_{20/24}$ the thermocline depth and τ_x the zonal wind stress. Upwelling and mixing of thermocline temperature anomalies are parametrized by α. The finite upwelling time δ is prescribed from observations [*Zelle et al.*, 2004] and varies from less than one month east of 130°W to 5 months at the date line; this also agrees well with lag correlations of model data. The parameter β describes the effects of zonal advection, upwelling, evaporation and variations in mixed-layer depth on SST, neglecting nonlinear terms. The damping parameter γ includes cloud feedback in the western Pacific. Although the linear model fits the SST evolution well, nonlinear effects that are not included in equation (1), are known to play a role, especially in the central Pacific [e.g., *Boulanger et al.*, 2001].

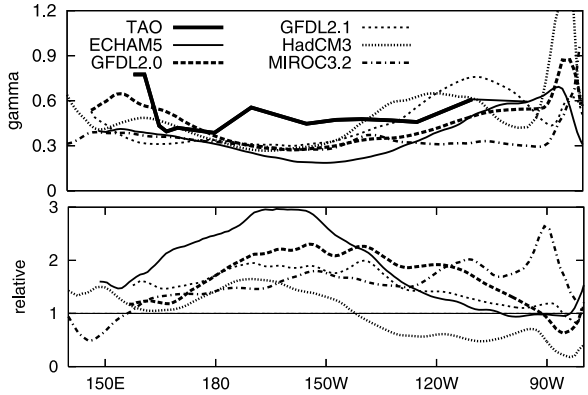

Figure 4. Damping term γ [month^{-1}] for the 20c3m scenario and the relative change in the warmer climate.

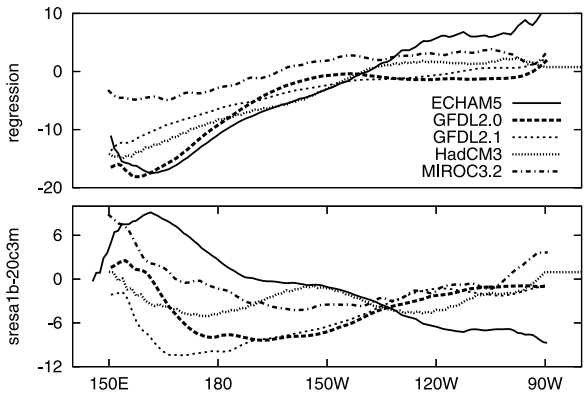

Figure 5. (top) Regression of the downward shortwave radiation with local SST, averaged over 5°S–5°N in the 20th century and (bottom) absolute difference between the 23rd and 20th centuries.

[17] Results for the current climate are presented by *Van Oldenborgh et al.* [2005]. These results are now compared to the sensitivities of SST in a doubled CO_2 scenario. The fitted coefficients of the linear SST equation in the current climate and the relative change between the current and the future climate are shown in Figures 2–4. Statistical uncertainties of the fitted parameters are in the order of 10% in the regions where they are the most important.

[18] The influence of thermocline depth variations is most important in the east Pacific where the thermocline is shallowest. The sensitivity to the thermocline depth, α (see Figure 2), becomes about two times higher in all models except in the HadCM3 model. The overall higher sensitivities in the models can be related to the shoaling of the thermocline as a whole (Figure 1). A shallower thermocline exerts a larger influence on SST. For HadCM3 the shoaling is not as clear as for the other models.

[19] Figure 3 shows β, the sensitivity of SST to wind stress, which is most important in the central Pacific. Almost all models show an increase in sensitivity to wind stress variability, especially in the central Pacific. The increased sensitivity of SST on wind stress may be related to the shallower oceanic MLD in a warmer climate (see Figure 1).

[20] All models show an increase in the damping term γ in the central Pacific (see Figure 4). This is partly due to a shift of the convection to the central Pacific, since at higher temperatures clouds extend more to the east, see Figure 5. For HadCM3 the change in the latent heat flux is equally important. ECHAM5 is an exception with no change in cloud-cover feedback in the central Pacific.

[21] Overall, we find roughly a doubling of the coupling strengths and damping in the areas where they are most important.

4.2. Zonal Wind Stress Response to SST Variability

[22] Another important feedback in the ENSO cycle is the response of the wind to SST anomalies along the equator. A change in this response influences the properties of the ENSO cycle. This wind sensitivity to SST anomalies is examined with a statistical atmosphere model with as basis n equal-sized boxes along the equator in 5°S–5°N, 140°E–80°W [e.g., *Von Storch and Zwiers*, 2001, section

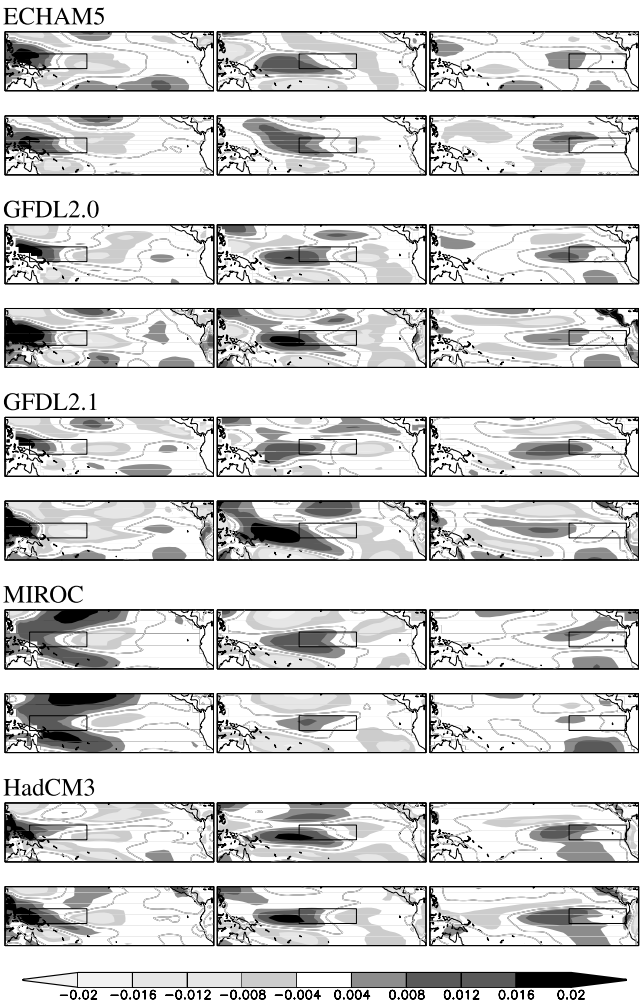

Figure 6. Wind response to SST anomalies in 120°E–70°W, 20°S–20°N for three boxes. Top plots are current climate, and bottom plots are doubled CO_2 climate.

8.3]. The model is defined as the response of the atmosphere on a SST anomaly in one of the boxes only. In this study we compare the atmospheric response to SST anomalies in $n = 3$ boxes separately for the climate of the 20th century and the doubled CO_2 scenario. The central box corresponds approximately to NINO4, the eastern box to NINO3 and the patterns are clear enough to study with one ensemble member for all five models.

[23] In our models the change in wind response to SST anomalies along the equator is consistent with the change in mean SST for the most localized warmings (see Figure 6 and *Liu et al.* [2005], Figure 1): GFDL2.0 and GFDL2.1 have a stronger maximum wind stress response of 100% and 30%, respectively, in the central Pacific where the SST rises the most. In the eastern Pacific the wind response reduces somewhat. ECHAM5 has a stronger response in the east (50%) where the SST also rises the most, and a weaker response in the central part (−20%). In HadCM3, where warming is about equal along the whole equator, the wind response is higher along the whole equator. The decrease in wind response is strongest in MIROC3.2 where the rise in SST is almost the same in all NINO regions.

[24] Overall, wind response to SST variability increases where the mean SST has increased most, but decreases where SST increases less. This is a combination of two effects. First, a warmer background temperature provides higher evaporation and a stronger wind response. This explains the spatial pattern of the changes. Second, the response as a function of a heating anomaly becomes about two times weaker everywhere along the equator in a doubled CO_2 climate (not shown). This can be attributed to the fact that the equatorial atmosphere becomes more stable.

5. Conclusions

[25] A previous study of El Niño in a future, warmer climate showed only small changes between the climate of the 20th century and a warmer climate in overall properties like period and amplitude of ENSO. It is tempting to conclude that El Niño will not change significantly. However, it was not clear how to interpret this result since the overall properties of the projected warmer climate differ clearly from the 20th century.

[26] In this study we show that although the overall ENSO properties do not change much, ENSO couplings are very different. In five GCMs with most reliable physics related to El Niño, the feedback loop between SST, wind stress and thermocline does change in greenhouse warming simulations following changes in the mean state. The mean SST, wind stress and thermocline show changes in the same direction. The mean SST increases more in the tropics than in the subtropics. The mean wind stress decreases and the convection cell shifts eastward. In the ocean the thermocline becomes shallower.

[27] These changes in mean states affect the feedback loop in these five GCMs as follows. SST sensitivity to thermocline variability increases since the thermocline is shallower, and the response of SST to wind stress becomes larger partly due to the decreased mixed layer depth. On the other hand, the higher mean SST provides higher damping through cloud feedback. The response of the wind stress to SST variability becomes only stronger near locations where the mean SST has increased the most. This is the result of the local higher background temperature, which increases the response of the wind stress on SST, counteracted by the overall lower response of wind on heating, which decreases the response of the wind stress. All these changes are visible in at least four of the five GCMs, although their location and precise strength differ. Besides these main factors other (nonlinear) mechanisms undoubtedly also play a role.

[28] We see that these changes impact with large amplitudes on the overall properties, but with opposing signs. The residual change is almost zero and depends on the details of ENSO in the GCMs.

[29] **Acknowledgments.** We acknowledge the international modeling groups for providing their data for analysis, the Program for Climate Model Diagnosis and Intercomparison for collecting and archiving the model data, the JSC/CLIVAR Working Group on Coupled Modelling and their Coupled Model Intercomparison Project and Climate Simulation Panel for organizing the model data analysis activity, and the IPCC WG1 TSU for technical support. The IPCC Data Archive at Lawrence Livermore National Laboratory is supported by the Office of Science, US Department of Energy. We kindly thank Noel Keenlyside for providing the data for ECHAM5/MPI-OM. Matthew Collins and Thomas Toniazzo are thanked for comments and suggestions. This research is supported by the Research

Council for Earth and Life Sciences (ALW) of the Netherlands Organisation for Scientific Research (NWO).

References

Boulanger, J.-P., E. Durand, J.-P. Duvel, C. Menkes, P. Delecluse, M. Imbard, M. Lengaigne, and S. Masson (2001), Role of non-linear ocean processes to westerly wind events: New implications for the 1997 El Niño onset, *Geophys. Res. Lett.*, *28*, 1603–1606.

Burgers, G. J. H., and G. J. van Oldenborgh (2002), On the impact of local feedbacks in the central Pacific on the ENSO cycle, *J. Clim.*, *16*, 2396–2407.

Capotondi, A., A. Wittenberg, and S. Masina (2006), Spatial and temporal structure of ENSO in 20th century coupled simulations, *Ocean Modell.*, in press.

Guilyardi, E. (2006), El Niño-mean state-seasonal cycle interactions in a multi-model ensemble, *Clim. Dyn.*, *26*, 329–348.

Kirtman, B. (1997), Oceanic Rossby wave dynamics and the ENSO period in a coupled model, *J. Clim.*, *10*, 1690–1704.

Liu, Z., S. Vavrus, F. He, N. Wen, and Y. Zhong (2005), Rethinking tropical ocean response to global warming: The enhanced equatorial warming, *J. Clim.*, *18*, 4684–4700.

McPhaden, M. J., et al. (1998), The Tropical Ocean Global Atmosphere (TOGA) observing system: A decade of progress, *J. Geophys. Res.*, *103*, 14,169–14,240.

Merryfield, W. J. (2006), Changes in ENSO under CO_2 doubling in the IPCC AR4 coupled climate models, *J. Clim.*, in press.

Toniazzo, T. (2006), Properties of the El Niño Southern Oscillation in different equilibrium climates with the HadCM3 model, *J. Clim.*, in press.

Van Oldenborgh, G. J., S. Y. Philip, and M. Collins (2005), El Niño in a changing climate: A multi-model study, *Ocean Sci.*, *1*, 81–95.

Von Storch, H., and F. Zwiers (2001), *Statistical Analysis in Climate Research*, 84 pp., Cambridge Univ. Press, New York.

Zelle, H., G. Appeldoorn, G. Burgers, and G. J. van Oldenborgh (2004), On the relationship between sea surface temperature and thermocline depth in the eastern equatorial Pacific, *J. Phys. Oceanogr.*, *34*, 643–655.

Zelle, H., G. J. Van Oldenborgh, G. Burgers, and H. A. Dijkstra (2005), El Niño and greenhouse warming: Results from ensemble simulations with the NCAR CCSM, *J. Clim.*, *18*, 4669–4683.

S. Y. Philip and G. J. van Oldenborgh, Royal Netherlands Institute of Meteorology, P.O. Box 201, NL-3730 AE De Bilt, Netherlands. (philip@knmi.nl; oldenborgh@knmi.nl)